

Comparison between Fermion Bag Approach and Complex Langevin Dynamics for Massive Thirring Model at Finite Density in 0 + 1 Dimensions

Daming Li*

School of Mathematical Sciences, Shanghai Jiao Tong University, Shanghai, 200240, China

Abstract

We consider the massive Thirring model at finite density in 0+1 dimension. The fermion bag approach, Langevin dynamics and complex Langevin dynamics are adopted to attack the sign problem for this model. Compared with the complex Langevin dynamics, both fermion bag approach and Langevin dynamics avoid the sign problem. The fermion density and chiral condensate, which are obtained by these numerical methods, are compared with the exact results. The advantages of the fermion bag approach over the other numerical methods are also discussed.

Keywords: Thirring model, finite density, complex Langevin dynamics, fermion bag approach

PACS: 05.50.+q, 71.10.Fd, 02.70.Ss

1. Introduction

The usual sampling methods, e.g., Langevin dynamics and Monte Carlo method, fail for the complex action, since the Boltzmann factor can not be regarded as the probability density. This problem, called the sign problem, is still the main obstacle of the computation in lattice quantum field. Three reasons will always lead to the complex action: (1) grand partition function with finite density; (2) fermion systems; (3) topological terms in the action.

To overcome the sign problem, the complex Langevin dynamics, which is obtained from the complexification of the Langevin dynamics, was used, which is rather successful in XY model [1], Bose gas [2], Thirring model [3], Abelian and Non-Abelian lattice gauge model [4], QCD model [5], and its simplified model including one link U(1) model, one link SU(3) model, QCD model in the heavy mass limit [6], one link SU(N) model [7], SU(3) spin model [8], Polykov chain model [9]. For some range of chemical potential μ and large fluctuation, the complex Langevin may fails, e.g., the XY model at finite chemical potential for

*Corresponding author

Email address: lidaming@sjtu.edu.cn (Daming Li)

small β (large fluctuation) [10] and in the Thirring model in 0+1 dimension [11]. Unfortunately from early studies of complex Langevin evolutions [12][13][14] until this day, the convergence properties of complex Langevin equations are not well understood. Recently Aarts etc. provided a criterion for checking the correctness of the complex Langevin dynamics [15].

It is possible to find suitable variables to represent the partition function such that the action is real. This is called the dual variable method. It is successfully applied to many models, including Bose gas [16], SU(3) spin model [17], U(1) and Z(3) gauge Higgs lattice theory [18], massive lattice Schwinger model [19], O(3), O(N) and CP(N-1) model [20][21][22][23], fermion bag approach [24], 4-fermion lattice theory, including massless Thirring model [25], Gross-Neveu model [26], Yukawa model [27], Non-Abelian Yang-Mills model [28][29], and its coupling with fermion field [30], lattice chiral model, and Sigma model [31]. Although the routine to find the dual variable is case by case, its technique behind is based on the high temperature expansion. For the fermion system, the dual method is called fermion bag approach [24]. This numerical method not only overcome the sign problem for model with small chemical potential, but also a high computational efficiency is achieved for the small or large coupling between the fermions. In this paper we compare the Langevin dynamics, the complex Langevin dynamics and the fermion bag approach for the massive Thirring model at finite density in 0+1 dimension. The chiral condensate and fermion density obtained by these two numerical methods, are compared with the exact result.

The arrangement of the paper is as follows. In section 2, the Fermion bag approach for Thirring model is presented. In section 3, the complex Langevin dynamics and (real) Langevin dynamics are given for this model by introducing a bosonic variable. In section 4, the implementation of these numerical methods are presented, and are compared with the exact result. Conclusions are given in section 5.

2. Thirring model in 0+1 dimension

The lattice partition function for the massive Thirring model at the finite density in 0+1 dimension reads

$$Z = \int d\bar{\psi}d\psi e^{-S} \quad (1)$$

where $d\bar{\psi}d\psi = \prod_{t=0}^{N-1} d\bar{\psi}_t d\psi_t$ is the measure of the Grassmann fields $\psi = \{\psi_t\}_{t=0}^{N-1}$ and $\bar{\psi} = \{\bar{\psi}_t\}_{t=0}^{N-1}$, with even number of sites N . We adopt anti-periodic condition for ψ and $\bar{\psi}$

$$\psi_N = -\psi_0, \quad \psi_{-1} = -\psi_{N-1}, \quad \bar{\psi}_N = -\bar{\psi}_0, \quad \bar{\psi}_{-1} = -\bar{\psi}_{N-1}$$

The staggered fermion action S is

$$S = \sum_{t,\tau=0}^{N-1} \bar{\psi}_t D_{t,\tau} \psi_\tau - U \sum_{t=0}^{N-1} \bar{\psi}_t \psi_t \bar{\psi}_{t+1} \psi_{t+1} \quad (2)$$

Here $t + 1$ is always understood to be $(t + 1) \bmod N$, which becomes 0 if $t = N - 1$ since the period is N . The coupling constant U between fermions is nonnegative. The fermion matrix D is

$$D_{t,\tau} = D(\mu, m)_{t,\tau} = \frac{1}{2} \left(s_t^1 e^\mu \delta_{t+1,\tau} - s_t^2 e^{-\mu} \delta_{t,\tau+1} \right) + m \delta_{t,\tau}, \quad 0 \leq t, \tau \leq N - 1$$

with the chemical potential μ and fermion mass m . The antiperiodic condition for the ψ and $\bar{\psi}$ are accounted for by the sign s^1 and s^2

$$s_t^1 = \begin{cases} -1 & \text{if } t = N - 1 \\ 1 & \text{if } 0 \leq t < N - 1 \end{cases}, \quad s_t^2 = \begin{cases} -1 & \text{if } t = 0 \\ 1 & \text{if } 1 \leq t \leq N - 1 \end{cases} \quad (3)$$

A periodic extension for s^1 and s^2 is used to define them for any t . Thus we have $s_t^1 = s_{t+1}^2$ for any t . By using this formula for D , the action S in (2) can be written as a sum over edges $(t, t + 1)$

$$\begin{aligned} S &= \frac{1}{2} e^\mu (\bar{\psi}_0 \psi_1 + \cdots + \bar{\psi}_{N-2} \psi_{N-1} + \bar{\psi}_{N-1} \psi_0) \\ &\quad + \frac{1}{2} e^{-\mu} (\psi_{N-1} \bar{\psi}_0 + \psi_0 \bar{\psi}_1 + \cdots + \psi_{N-2} \bar{\psi}_{N-1}) \\ &\quad + m \sum_{t=0}^{N-1} \bar{\psi}_t \psi_t + U \sum_{t=0}^{N-1} (\bar{\psi}_t \psi_{t+1}) (\bar{\psi}_{t+1} \psi_t) \end{aligned}$$

It is easy to check the symmetry of the fermion matrix $D(\mu, m)$ with respect to μ and m

$$D(\mu, m)_{t,\tau} = -D(-\mu, -m)_{\tau,t} \implies \det D(\mu, m) = \det D(-\mu, -m) \quad (4)$$

$$\varepsilon D(\mu, m) \varepsilon = -D(\mu, -m) \implies \det D(\mu, m) = \det D(\mu, -m) \quad (5)$$

where $\varepsilon_{t,\tau} = \delta_{t,\tau} \varepsilon_t$, $\varepsilon_t = (-1)^t$. Thus it is enough to study $\mu \geq 0$ and $m \geq 0$ in the massive Thirring model.

The idea of the fermion bag approach is to expand the Boltzmann factor e^{-S} by the high temperature expansion,

$$\begin{aligned} \exp(-S) &= \exp \left(- \sum_{t,\tau=0}^{N-1} \bar{\psi}_t D_{t,\tau} \psi_\tau \right) \prod_{t=0}^{N-1} \exp \left(U \bar{\psi}_t \psi_t \bar{\psi}_{t+1} \psi_{t+1} \right) \\ &= \exp \left(- \sum_{t,\tau=0}^{N-1} \bar{\psi}_t D_{t,\tau} \psi_\tau \right) \prod_{t=0}^{N-1} \sum_{k_t=0}^1 (U \bar{\psi}_t \psi_t \bar{\psi}_{t+1} \psi_{t+1})^{k_t} \quad (6) \end{aligned}$$

and the partition function Z is written as the sum over the configuration $k = (k_t = 0, 1)_{t=0}^{N-1}$

$$Z = \sum_k U^j C(t_1, \cdots, t_{2j}) \quad (7)$$

where $k_t = 0, 1$ for all two neighboring sites $(t, t+1)$, which satisfies $k_{t-1} + k_t \leq 1$ for all site t . If $k_t = 1$, we say there is a bond connecting t and $t+1$; otherwise, there are no bonds connecting them. For given configuration k , for example, there are j bonds $(t_1, t_2), \dots, (t_{2j-1}, t_{2j})$ connecting $2j$ different sites (t_1, \dots, t_{2j}) . For such kind of configuration k , C in (7) is given by

$$\begin{aligned} C(t_1, \dots, t_{2j}) &= \int d\bar{\psi}d\psi \exp\left(-\sum_{t,\tau=0}^{N-1} \bar{\psi}_t D_{t,\tau} \psi_\tau\right) \bar{\psi}_{t_1} \psi_{t_1} \cdots \bar{\psi}_{t_{2j}} \psi_{t_{2j}} \quad (8) \\ &= \det D \det G(\{t_1, \dots, t_{2j}\}) = \det D(\setminus\{t_1, \dots, t_{2j}\}) \end{aligned}$$

where $G(\{t_1, \dots, t_{2j}\})$ is a $(2j) \times (2j)$ matrix of propagators between $2j$ sites t_i , $i = 1, \dots, 2j$, whose matrix element are $G(\{t_1, \dots, t_{2j}\})_{i,l} = D_{t_i, t_l}^{-1}$, $i, l = 1, \dots, 2j$. The matrix $G(\{t_1, \dots, t_{2j}\})$ depends on the order of $\{t_1, \dots, t_{2j}\}$, but it's determinant does not. $D(\setminus\{t_1, \dots, t_{2j}\})$ is the $(N-2j) \times (N-2j)$ matrix which is obtained by deleting rows and columns corresponding to sites t_1, \dots, t_{2j} . Thus if j is small, we use $G(\{t_1, \dots, t_{2j}\})$ to calculate $C(t_1, \dots, t_{2j})$; otherwise, we adopted $D(\setminus\{t_1, \dots, t_{2j}\})$ to calculate $C(t_1, \dots, t_{2j})$. Because of the symmetry (4) and (5) of D , it is easy to show that for any μ, m and any number of different sites t_1, \dots, t_n

$$\begin{aligned} C(t_1, \dots, t_n; D(\mu, m)) &= (-1)^n C(t_1, \dots, t_n; D(\mu, -m)) \\ &= C(t_1, \dots, t_n; D(-\mu, m)) = (-1)^n C(t_1, \dots, t_n; D(-\mu, -m)) \quad (9) \end{aligned}$$

where $C(t_1, \dots, t_n; D(\mu, m))$ denote the function C in (8) since it depends on the fermion matrix $D(\mu, m)$. We can rigorously prove that for any $\mu \geq 0$ and $m > 0$, $C(t_1, \dots, t_j) > 0$ for any number of different sites $\{t_i\}_{i=1}^j$ (Appendix A). Thus the sign problem is avoided by the presentation (7) of the partition function for the massive Thirring model with finite density in 0+1 dimensions.

The chiral condensate is

$$\langle \bar{\psi}\psi \rangle = \frac{1}{N} \frac{\partial \ln Z}{\partial m} = \frac{1}{N} \left\langle \frac{\partial_m C(t_1, \dots, t_{2j})}{C(t_1, \dots, t_{2j})} \right\rangle \quad (10)$$

where the average is taken with respect to the weight of the partition function (7). From the first line in (9), $C(t_1, \dots, t_{2j})$ is even in m and the chiral condensate $\langle \bar{\psi}\psi \rangle$ vanishes if $m = 0$. Similar to the calculation of C in (8), we also have two methods to calculate its partial derivative $\partial_m C$

$$\begin{aligned} \partial_m C(t_1, \dots, t_{2j}) &= \sum_{t \neq t_1, \dots, t_{2j}} \det D \det G(\{t, t_1, \dots, t_{2j}\}) \\ &= \sum_{t \neq t_1, \dots, t_{2j}} \det D(\setminus\{t, t_1, \dots, t_{2j}\}) \quad (11) \end{aligned}$$

The fermion density is

$$\langle n \rangle = \frac{1}{N} \frac{\partial \ln Z}{\partial \mu} = \frac{1}{N} \left\langle \frac{\partial_\mu C(t_1, \dots, t_{2j})}{C(t_1, \dots, t_{2j})} \right\rangle \quad (12)$$

which vanishes if $\mu = 0$ since $C(t_1, \dots, t_{2j})$ is even in μ by (9). The partial derivative of C with respect to μ is

$$\begin{aligned} & \partial_\mu C(t_1, \dots, t_{2j}) \\ = & \sum_{t, t+1 \neq t_1, \dots, t_{2j}} \frac{1}{2} e^\mu s_t^1 \det D \det G[(t_1, \dots, t_{2j}, t+1), (t_1, \dots, t_{2j}, t)] + \\ & \sum_{t, t-1 \neq t_1, \dots, t_{2j}} \frac{1}{2} e^{-\mu} s_t^2 \det D \det G[(t_1, \dots, t_{2j}, t-1), (t_1, \dots, t_{2j}, t)] \end{aligned}$$

where the $(2j+1) \times (2j+1)$ propagator matrix $G[(t_1, \dots, t_{2j}, t \pm 1), (t_1, \dots, t_{2j}, t)]$ has (i, l) matrix element D_{t_i, τ_l}^{-1} , $i, l = 1, \dots, 2j+1$. Here we use notations $t_{2j+1} \equiv t \pm 1$, $\tau_l = t_l$, $l = 1, \dots, 2j$, $\tau_{2j+1} = t$. The ratio in (12) is

$$\begin{aligned} & \frac{\partial_\mu C(t_1, \dots, t_{2j})}{C(t_1, \dots, t_{2j})} \\ = & \frac{1}{2} e^\mu \sum_{t, t+1 \neq t_1, \dots, t_{2j}} s_t^1 \frac{\det G[(t_1, \dots, t_{2j}, t+1), (t_1, \dots, t_{2j}, t)]}{\det G[(t_1, \dots, t_{2j}), (t_1, \dots, t_{2j})]} + \\ & \frac{1}{2} e^{-\mu} \sum_{t, t-1 \neq t_1, \dots, t_{2j}} s_t^2 \frac{\det G[(t_1, \dots, t_{2j}, t-1), (t_1, \dots, t_{2j}, t)]}{\det G[(t_1, \dots, t_{2j}), (t_1, \dots, t_{2j})]} \end{aligned}$$

Note that $G[(t_1, \dots, t_{2j}), (t_1, \dots, t_{2j})] = G(\{t_1, \dots, t_{2j}\})$. The ratio between the determinant can be obtained by

$$\begin{aligned} & \frac{\det G[(t_1, \dots, t_{2j}, t \pm 1), (t_1, \dots, t_{2j}, t)]}{\det G[(t_1, \dots, t_{2j}), (t_1, \dots, t_{2j})]} = G[(t \pm 1), (t)] \\ & - G[(t \pm 1), \text{occu_sites}] G[\text{occu_sites}, \text{occu_sites}]^{-1} G[\text{occu_sites}, (t)] \end{aligned}$$

where $\text{occu_sites} = (t_1, \dots, t_{2j})$ denotes $2j$ occupied sites. $G[\text{occu_sites}, \text{occu_sites}]$ is the $2j \times 2j$ propagator matrix with (i, l) matrix element D_{t_i, t_l}^{-1} , $i, l = 1, \dots, 2j$. Another form of $\partial_\mu C$ is

$$\begin{aligned} & \partial_\mu C(t_1, \dots, t_{2j}) \\ = & \frac{1}{2} e^\mu \sum_{t, t+1 \neq t_1, \dots, t_{2j}} s_t^1 (-1)^{(t)-(t+1)} \det D[\setminus(t_1, \dots, t_{2j}, t), \setminus(t_1, \dots, t_{2j}, t+1)] + \\ & \frac{1}{2} e^{-\mu} \sum_{t, t-1 \neq t_1, \dots, t_{2j}} s_t^2 (-1)^{(t)-(t-1)} \det D[\setminus(t_1, \dots, t_{2j}, t), \setminus(t_1, \dots, t_{2j}, t-1)] \end{aligned}$$

where (t) and $(t+1)$ denote the position of t and $t+1$ in the $N-2j$ $\text{free_sites} = \setminus\{t_1, \dots, t_{2j}\}$, respectively. $D[\setminus(t_1, \dots, t_{2j}, t), \setminus(t_1, \dots, t_{2j}, t \pm 1)]$ denotes the $(N-2j-1) \times (N-2j-1)$ matrix obtained from D by deleting rows (t_1, \dots, t_{2j}, t)

and columns $(t_1, \dots, t_{2j}, t \pm 1)$. Using this formula, one has

$$\begin{aligned} & \frac{\partial_\mu C(t_1, \dots, t_{2j})}{C(t_1, \dots, t_{2j})} \\ = & \frac{1}{2} e^\mu \sum_{t, t+1 \neq t_1, \dots, t_{2j}} s_t^1 (-1)^{(t)-(t+1)} \frac{\det D[\setminus(t_1, \dots, t_{2j}, t), \setminus(t_1, \dots, t_{2j}, t+1)]}{\det D[\setminus(t_1, \dots, t_{2j}), \setminus(t_1, \dots, t_{2j})]} + \\ & \frac{1}{2} e^{-\mu} \sum_{t, t-1 \neq t_1, \dots, t_{2j}} s_t^2 (-1)^{(t)-(t-1)} \frac{\det D[\setminus(t_1, \dots, t_{2j}, t), \setminus(t_1, \dots, t_{2j}, t-1)]}{\det D[\setminus(t_1, \dots, t_{2j}), \setminus(t_1, \dots, t_{2j})]} \end{aligned}$$

Note that $D[\setminus(t_1, \dots, t_{2j}), \setminus(t_1, \dots, t_{2j})] = D[\setminus\{t_1, \dots, t_{2j}\}]$. The ratio between the determinant is

$$(-1)^{(t)-(t\pm 1)} \frac{\det D[\setminus(t_1, \dots, t_{2j}, t), \setminus(t_1, \dots, t_{2j}, t \pm 1)]}{\det D[\setminus(t_1, \dots, t_{2j}), \setminus(t_1, \dots, t_{2j})]} = \text{D_Inv}[(t \pm 1), (t)]$$

where $\text{D_Inv}[(t \pm 1), (t)]$ is the $(t \pm 1, t)$ matrix element of $(N-2j) \times (N-2j)$ matrix D_Inv , which is the inverse of $(N-2j) \times (N-2j)$ matrix $D[\text{free_sites}, \text{free_sites}]$.

The Monte Carlo algorithm based on the partition function in (7) can be found in Ref.[25]. We adopt the following steps to update the current configuration. Assume that the current configuration k has n_b bonds

$$C = ([t_1, t_2], \dots, [t_{2n_b-1}, t_{2n_b}])$$

Try to delete a bond, e.g. $[t_{2n_b-1}, t_{2n_b}]$ from the current configuration C to be

$$C' = ([t_1, t_2], \dots, [t_{2n_b-3}, t_{2n_b-2}])$$

According to the detailed balance

$$W(C)P_{try}(C \rightarrow C')P_{acc}(C' \rightarrow C) = W(C')P_{try}(C' \rightarrow C)P_{acc}(C \rightarrow C') \quad (13)$$

where $W(C)$ and $W(C')$ are the weight in the partition function (7) for the configuration C and C' , respectively. The try probability from $C(C')$ to $C'(C)$ are

$$P_{try}(C \rightarrow C') = \frac{1}{n_b}, \quad P_{try}(C' \rightarrow C) = \frac{1}{n_f}$$

respectively. Here n_f is the number of bonds which can be created from the configuration C' . Thus the accept probability from C to C' is

$$P_{acc}(C \rightarrow C') = \frac{n_b}{n_f} \frac{W(C')}{W(C)}$$

Try to add a bond, e.g. $[t_{2n_b+1}, t_{2n_b+2}]$ from the current configuration C to be

$$C' = ([t_1, t_2], \dots, [t_{2n_b-1}, t_{2n_b}], [t_{2n_b+1}, t_{2n_b+2}])$$

The detailed balance is Eq. (13) where

$$P_{try}(C \rightarrow C') = \frac{1}{n_f}, \quad P_{try}(C' \rightarrow C) = \frac{1}{n_b + 1}$$

Here n_f is the number of bonds which can be created from the configuration C . Thus the accept probability from C to C' is

$$P_{acc}(C \rightarrow C') = \frac{n_f}{n_b + 1} \frac{W(C')}{W(C)}$$

Try to delete a bond, e.g. $[t_{2n_b-1}, t_{2n_b}]$ from the current configuration C and then add a bond, e.g., $[y_{2n_b-1}, y_{2n_b}]$ to be

$$C' = ([t_1, t_2], \dots, [t_{2n_b-3}, t_{2n_b-2}], [y_{2n_b-1}, y_{2n_b}])$$

In the detailed balance (13),

$$P_{try}(C \rightarrow C') = P_{try}(C' \rightarrow C) = \frac{1}{n_b n_f}$$

Here n_f is the number of bonds which can be created from the configuration C where $[t_{2n_b-1}, t_{2n_b}]$ is deleted. Thus the accept probability to move a bond is

$$P_{acc}(C \rightarrow C') = \frac{W(C')}{W(C)}$$

3. Complex Langevin dynamics

The Grassmann fields $\bar{\psi}$ and ψ can be eliminated if an bosonic variable A_t are introduced

$$\begin{aligned} \exp\left(U \sum_{t=0}^{N-1} \bar{\psi}_t \psi_t \bar{\psi}_{t+1} \psi_{t+1}\right) &= \int \prod_{t=0}^{N-1} dA_t \exp\left(-\frac{1}{8U} \sum_{t=0}^{N-1} A_t^2\right) \\ \exp\left(-\sum_{t,\tau=0}^{N-1} \bar{\psi}_t \frac{i}{2} (e^\mu A_t \delta_{t+1,\tau} + e^{-\mu} A_\tau \delta_{t,\tau+1}) \psi_\tau\right) & \end{aligned} \quad (14)$$

where we omit a term depending on U . Inserting this formula to the partition function Z in (1) and integrating over the Grassmann fields, one has

$$Z = \int \prod_{t=0}^{N-1} dA_t \exp\left(-\frac{1}{8U} \sum_{t=0}^{N-1} A_t^2\right) \det K = \int \prod_{t=0}^{N-1} dA_t e^{-S_{\text{eff}}} \quad (15)$$

where the $N \times N$ fermion matrix K under the bosonic variable A is

$$K_{t,\tau} = \frac{1}{2} \left((s_t^1 + iA_t) e^\mu \delta_{t+1,\tau} - (s_t^2 - iA_\tau) e^{-\mu} \delta_{t,\tau+1} \right) + m \delta_{t,\tau} \quad (16)$$

for $0 \leq t, \tau \leq N - 1$. The fermion matrix K becomes the fermion matrix D if $A = 0$. This form of partition function in (15) was studied in Ref.[11]. The effective action in (15) is

$$S_{\text{eff}} = \frac{1}{8U} \sum_{t=0}^{N-1} A_t^2 - \ln \det K \quad (17)$$

is complex. The discrete complex Langevin dynamics for (15)

$$A_{t,\Theta+\Delta\Theta} = A_{t,\Theta} - \Delta\Theta \frac{\partial S_{\text{eff}}}{\partial A_{t,\Theta}} + \sqrt{2\Delta\Theta} \eta_{t,\Theta}, \quad 0 \leq t \leq N - 1, \quad \Theta = 0, 1, \dots \quad (18)$$

where Θ denotes the discrete complex Langevin time, $\Delta\Theta$ is the time step. The real white noise $\eta_{t,\Theta} \sim \mathcal{N}(0, 1)$ satisfies

$$\langle \eta_{t,\Theta} \eta_{\tau,\Theta'} \rangle = \delta_{t,\tau} \delta_{\Theta,\Theta'}$$

Since S_{eff} is complex, $A_{t,\Theta}$ is also complex. Using (16) and (17), the drift force in (18) is

$$-\frac{\partial S_{\text{eff}}}{\partial A_t} = -\frac{1}{4U} A_t + \frac{i}{2} \left(e^\mu K_{t+1,t}^{-1} + e^{-\mu} K_{t,t+1}^{-1} \right) \quad (19)$$

The chiral condensate in (10) is written as

$$\langle \bar{\chi} \chi \rangle = \frac{1}{N} \langle \text{Tr}(K^{-1}) \rangle \quad (20)$$

and the fermion density in (12) reads

$$\langle n \rangle = \frac{1}{N} \left\langle \text{Tr} \left(K^{-1} \frac{\partial K}{\partial \mu} \right) \right\rangle \quad (21)$$

Here the average is taken with respect to weight $e^{-S_{\text{eff}}}$.

The equation (14) is also valid if A_t and A_τ are replaced by $s_t^1 A_t$, $s_t^2 A_\tau$, respectively. The partition function Z is

$$Z = \int \prod_{t=0}^{N-1} dA_t \exp \left(-\frac{1}{8U} \sum_{t=0}^{N-1} A_t^2 \right) \det \tilde{K} \quad (22)$$

where the $N \times N$ fermion matrix \tilde{K} under the bosonic variable A is

$$\tilde{K}_{t,\tau} = \frac{1}{2} \left(s_t^1 (1 + iA_t) e^\mu \delta_{t+1,\tau} - s_t^2 (1 - iA_\tau) e^{-\mu} \delta_{t,\tau+1} \right) + m \delta_{t,\tau} \quad (23)$$

for $0 \leq t, \tau \leq N - 1$. Fortunately the determinant of \tilde{K} can be calculated by [33]

$$\det \tilde{K} = \frac{e^{N\mu}}{2^N} \prod_{t=0}^{N-1} (1 + iA_t) + \frac{e^{-N\mu}}{2^N} \prod_{t=0}^{N-1} (1 - iA_t) + \text{Tr}(T) \quad (24)$$

where the 2×2 transfer matrix T is

$$T(A_0, \dots, A_{N-1}) = \begin{pmatrix} m & \frac{1}{4}(1 + A_0^2) \\ 1 & 0 \end{pmatrix} \dots \begin{pmatrix} m & \frac{1}{4}(1 + A_{N-1}^2) \\ 1 & 0 \end{pmatrix} \quad (25)$$

Inserting (24) into the partition function Z in (22), one has $Z = Z_1(\mu) + Z_2(m)$ where

$$Z_1(\mu) = 2(2\pi U)^{N/2} \cosh(N\mu), \quad Z_2(m) = \int \prod_{t=0}^{N-1} dA_t \exp\left(-\frac{1}{8U} \sum_{t=0}^{N-1} A_t^2\right) \text{Tr}(T)$$

The chiral condensate is

$$\langle \bar{\chi}\chi \rangle = \frac{1}{N} \frac{\langle \text{Tr}(\partial_m T) \rangle_0}{2^{-N} 2 \cosh(N\mu) + \langle \text{Tr}(T) \rangle_0} \quad (26)$$

where the average is taken with respect to the weight $\exp(-\frac{1}{8U} \sum_{t=0}^{N-1} A_t^2)$. The fermion density reads

$$\langle n \rangle = \frac{2 \sinh(N\mu)}{2 \cosh(N\mu) + 2^N \langle \text{Tr}(T) \rangle_0} \quad (27)$$

Since the observable $\text{Tr}(T) > 0$ and $\text{Tr}(\partial_m T) > 0$ for any real fields $\{A_t\}_{t=0}^{N-1}$, the sign problem in this representation is avoided. These averages $\langle \dots \rangle_0$ can be calculated by the usual Monte Carlo method or Langevin dynamics since these averages is taken over the Gaussian weight $\exp(-\frac{1}{8U} \sum_{t=0}^{N-1} A_t^2)$. We use (real) Langevin dynamics

$$A_{t,\Theta+\Delta\Theta} = A_{t,\Theta} - \Delta\Theta \frac{1}{4U} A_t + \sqrt{2\Delta\Theta} \eta_{t,\Theta}, \quad 0 \leq t \leq N-1, \quad \Theta = 0, 1, \dots \quad (28)$$

to calculate these averages. Here Θ denotes the discrete Langevin time and $\Delta\Theta$ is the time step. The real white noise $\eta_{t,\Theta} \sim \mathcal{N}(0, 1)$ satisfies $\langle \eta_{t,\Theta} \eta_{r,\Theta'} \rangle = \delta_{t,r} \delta_{\Theta,\Theta'}$. The averages $\langle \text{Tr}(T) \rangle_0$ and $\langle \text{Tr}(\partial_m T) \rangle_0$, which does not depend on the chemical potential μ , are obtained by samples $\{A_t\}_{t=0}^{N-1}$ after the equilibrium of the real Langevin dynamics. Moreover, the chiral condensate in (26) and fermion density in (27) can be obtained from $\langle \text{Tr}(T) \rangle_0$ and $\langle \text{Tr}(\partial_m T) \rangle_0$ for all chemical potential μ .

The computational complexity for the calculation of $\text{Tr}(T)$ and $\text{Tr}(\partial_m T)$ are $O(N)$, which will be explained in the next section. The exact formula for $Z_2(m)$ is known [11],

$$Z_2(m) = 2(2\pi U)^{N/2} (B_+ + B_-) \quad (29)$$

$$B_{\pm} = \frac{m^N}{2} \left(1 \pm \sqrt{4UB_c}\right)^N, \quad B_c = \frac{1}{4U} + \left(\frac{1}{4U} + 1\right) \frac{1}{m^2} \quad (30)$$

Thus these averages can be calculated exactly, which is called the exact result in the following sections.

4. Numerical results

4.1. Implementation

The most advantage of the fermion bag approach is that the weight in (7) is nonnegative and thus the sign problem is avoided in the interesting range of parameters, $0 \leq \mu \leq 2$, $0 < m < 100$, $0 \leq U \leq 10$. Table 1 shows the values of $C(t_1, \dots, t_j)$ for randomly chosen j sites t_1, \dots, t_j .

The Monte Carlo implementation for the fermion bag approach, including three steps of configuration updating and sampling of chiral condensate and fermion density, depends on the ratio of the value of C . For small coupling constant U , there are few bonds connecting neighboring sites, we use the propagation matrix on the occupied sites to calculate this ratio; For large coupling constant U , many bonds connecting to neighboring sites appear, we use the fermion matrix on the free sites to calculate this ratio. Thus high computational efficiency is achieved for the fermion bag approach with weak or strong coupling between fermions. In our code, we use `D_org` and `D_inv` to denote the fermion matrix D and its inverse matrix, respectively, which does not change in the whole run. `free_sites` = `\occu_sites` and `occu_sites` denote the free sites and occupied sites for the current configuration k . Denote by `D_Inv[free_sites]` the inverse of `D_org[free_sites]` and by `D_Org[occu_sites]` the inverse of `D_inv[occu_sites]`, respectively. Here `D_org[free_sites]` (`D_inv[occu_sites]`) denotes the submatrix of `D_org` (`D_inv`) with the rows and columns corresponding to `free_sites` (`occu_sites`). Thus depending on the number of occupied sites, `D_Inv` or `D_Org` changes during Monte Carlo updating.

The initial configuration for k is the one where there are no bonds. The sampling is taken after 1×10^6 Monte Carlo steps, where in each step at most two bonds change. To reduce the autocorrelation effects, two subsequent samples are separated by $10N$ Monte Carlo steps. The sampling is finished after 1×10^7 Monte Carlo steps, thus about $9 \times 10^6 / (10N)$ samples are taken for each Monte Carlo simulation.

The implementation of the complex Langevin dynamics (18) is rather simple. The initial condition for A is zero everywhere. We choose the time step $\Delta\Theta = 10^{-4}$. The sampling is taken after $t_{\text{equ}} = 20$ (i.e., $20/\Delta\Theta = 2 \times 10^5$ complex Langevin steps). To compare with the fermion bag approach, two subsequent samples are separated by 10 complex Langevin steps. The end time in the complex Langevin dynamics is $t_{\text{end}} = 40$, thus about $20 \times 10^6 / (10N)$ samples are taken for each complex Langevin simulation.

To calculate the sampling (26) with the computational complexity $O(N)$, we introduce

$$C_i = B_0 \cdots B_i, \quad i = 0, \dots, N-1, \quad D_i = B_{i+1} \cdots B_{N-1}, \quad i = 0, \dots, N-2$$

where $B_i = \begin{pmatrix} m & \frac{1}{4}(1 + A_i^2) \\ 1 & 0 \end{pmatrix}$, $i = 0, \dots, N-1$. Using the iteration

$$C_{i+1} = C_i B_{i+1}, \quad i = 0, \dots, N-2, \quad D_i = B_{i+1} D_{i+1}, \quad i = N-3, \dots, 0$$

t_1, \dots, t_j	$C(t_1, \dots, t_j)$
empty	11.65480
3	0.006890
3 6	0.018226
3 4 5	0.019760
1 2 6 7	0.005100
0 2 3 6 7	0.026000
0 1 2 4 6 7	0.010000
0 1 2 3 4 5 7	0.100000
0 1 2 3 4 5 6 7	1.000000

Table 1: The value of C for randomly chosen occupied sites (t_1, \dots, t_j) , $m = 0.1$, $\mu = 1.0$, $N = 8$.

we know that the computational complexity for calculating $\{C_i\}_{i=0}^{N-1}$ and $\{D_i\}_{i=0}^{N-2}$ is $O(N)$. The trace of T is $\text{Tr}(T) = \text{Tr}(C_{N-1})$ and

$$\text{Tr}(\partial_m T) = \text{Tr}(FD_0) + \sum_{i=1}^{N-2} \text{Tr}(FD_i C_{i-1}) + \text{Tr}(FC_{N-2}), \quad F = \begin{pmatrix} 1 & 0 \\ 0 & 0 \end{pmatrix}$$

We use the Γ method to estimate the error for the samples in each Monte Carlo simulation or complex Langevin dynamics [32]. A typical result is shown in Figure 2 where the statistical error for the complex Langevin dynamics are larger than those for the fermion bag approach if the chemical potential is close to 1.

4.2. Simulation results

The exact result is known for the massive Thirring model with one flavor in 0+1 dimension [11]. We first compare the chiral condensate obtained by the Langevin dynamics and exact result. Since the sign problem is avoided and the observable is positive, the Langevin dynamics (See Eq. (26)(27)(28)) should reproduce the exact result. Figure 1 shows the agreement between the chiral condensate obtained by the Langevin dynamics and exact results. In fact, the agreement between them are also achieved for the parameters: $m = 0.1, 1, 3, 100$, $U = 1/400, 1/12, 1/4, 10$, $\mu = 0, 0.2, 0.4, \dots, 2.0$.

Figure 2 shows the comparison between fermion bag approach, complex Langevin dynamics with the exact results. The chiral condensate and fermion density for fermion bag approach agree very well with the exact result in the range $0 \leq \mu \leq 2$. Compared with the fermion bag approach, the result obtained by complex Langevin dynamics agree with exact result for small or large μ . Moreover the statistical error becomes large for the complex Langevin dynamics in the intermediate value μ . Figure 3 shows that the fermion bag approach and complex Langevin dynamics agree with the exact results very well when U is decreased to be $U = 1/400$. Since the interaction between fermions is decreased, the statistical error is also small compared with those in Figure 2. When U increased, the simulation results obtained by complex Langevin dynamics is not

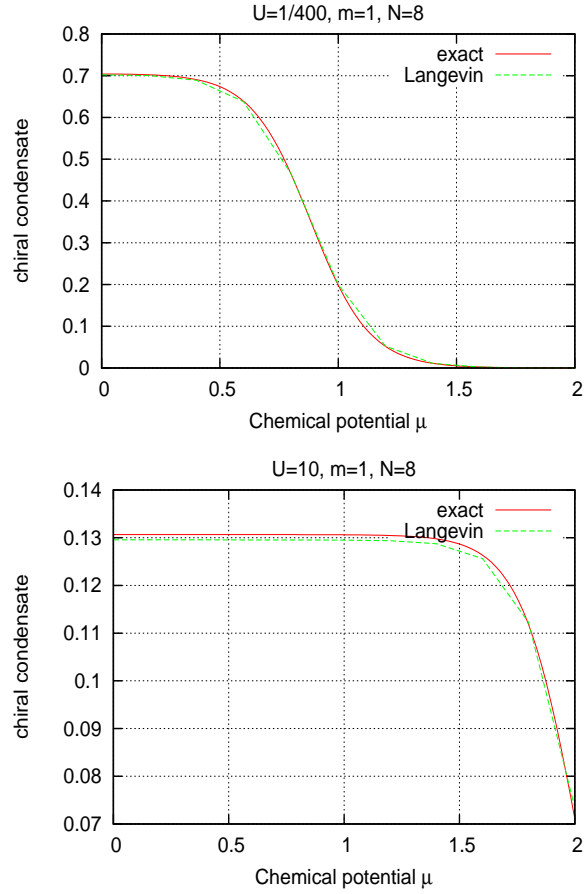


Figure 1: Comparison between Langevin dynamics and exact solution. Upper: $\Delta\Theta = 0.01$, $t_{\text{eq}} = 800$, $t_{\text{end}} = 1600$, $\langle\text{Tr}(T)\rangle_0 = 4.6145 \pm 0.000608$ and $\frac{1}{N}\langle\text{Tr}(\partial_m T)\rangle_0 = 3.2466 \pm 0.000369$. Bottom: $\Delta\Theta = 0.025$, $t_{\text{eq}} = 30000$, $t_{\text{end}} = 50000$, $\langle\text{Tr}(T)\rangle_0 = 45457.8 \pm 4456.4$ and $\frac{1}{N}\langle\text{Tr}(\partial_m T)\rangle_0 = 5888.6 \pm 405.1$.

reliable. According to Ref. [15][11], the quantity

$$\sum_{t=1}^N \left(\frac{d}{dA_t} - \frac{dS_{\text{eff}}}{dA_t} \right) \frac{d}{dA_t} O(A)$$

should vanish for any holomorphic function $O(A)$ if the complex Langevin dynamics works. We choose the observable (the chiral condensate) $O(A) = \frac{1}{N} \text{Tr}(K^{-1})$. For $\mu = 1$, $m = 1$ and $N = 8$, it is 0.0137 ± 0.00708 which is small if $U = 0.0025$ and becomes -5.88 ± 7.33 if $U = 0.16$. Moreover, the statistical error is also large which means that it is difficult to measure it reliably when U is increased. Figure 4 shows the dependence of the phase $\langle e^{i\varphi} \rangle_{\text{pq}} = Z/Z_{\text{pq}}$ on the coupling strength U for fixed chemical potential $\mu = 1$. Here Z_{pq} is the phase quenched approximation of Z in (15) where $\det K$ is replaced by its module $|\det K|$. When U is increased the phase $\langle e^{i\varphi} \rangle_{\text{pq}}$ decays to zero, which shows it suffers from a severe sign problem. Moreover, the statistic error is also increased if U becomes larger.

When $U = 10$, the results obtained by the fermion bag approach agree with exact result rather well, but the complex Langevin dynamics is totally wrong, which is shown in Figure 5. The failure of the complex Langevin dynamics for strong interaction was also found in Ref. [11]. For $\mu = 1.0$ in Figure 5, the average number of occupied bonds in the fermion bag approach is 3.41, which means almost all sites are occupied by bonds ($N = 8$). This leads to a slight difference of the chiral condensate obtained by the fermion bag approach and exact results. Figure 6 show that the average number of occupied bonds drops rapidly near $\mu = 2$ where the simulated results obtained by fermion bag approach agree with the exact result. Here we don't show the error bar in Figure 6 since it is very small which can be shown for the error bar of the chiral condensate by fermion bag approach in Figure 5. For fixed $m = 1$ and $\mu = 1$, 7 shows the dependence of the average number of occupied bonds (Left) and relative error for chiral condensate (Right) on the coupling strength U . The average number of occupied bonds increase with the coupling strength U . Since the exact solution is known, the relative error for the chiral condensate (obtained by the fermion bag approach) can be calculated as shown in the right figure of Figure 7 where the relative error is increased with the coupling strength when $U < 5$ or $U > 11$. We also notice there is an oscillation of the relative error for $6 < U < 11$. Thus if the coupling strength U is not too large the fermion bag approach can always reproduce the exact results. When U is very large, almost all lattice sites are occupied, which will lead a slight difference between results obtained by fermion bag approach and the exact results. It should be mentioned that the fluctuation of the chiral condensate and fermion density in the fermion bag approach is rather small even when U is rather large, e.g., $10 \leq U \leq 14$.

For the parameter: $U = 10$, $m = 1$ and $N = 8$, the chiral condensate obtained by Langevin dynamics in Figure 1 (bottom) and those by fermion bag approach in Figure 5 (upper) can reproduce the exact result. Compared with the fermion bag approach, the equilibrium time in the Langevin dynamics is very long. However, the advantage of the Langevin dynamics over the other

two approaches is that the chiral condensate and fermion density for any chemical potential can be obtained when the averages $\langle \text{Tr}(\partial_m T) \rangle_0$ and $\langle \text{Tr}(T) \rangle_0$ is calculated from the Langevin dynamics, since they do not depend on the chemical potential.

The comparison are also made between the fermion bag approach, complex Langevin dynamics with exact results in the range of parameters: $m = 0.1, 1, 3, 100$, $U = 1/400, 1/12, 1/4, 10$, $\mu = 0, 0.2, 0.4, \dots, 2.0$. The chiral condensate and fermion density obtained by the fermion bag approach agrees very well with the exact results for all these parameters. The reason is that the weight in the fermion bag approach is nonnegative and thus the sign problem is avoided. The results obtained by complex Langevin dynamics agree with the exact results only if U is not too large, $U < O(1)$. When U is increased, compared with the drift term, the white noise fluctuation in complex Langevin equation becomes large and thus the complex Langevin does not work, especially, when the fermion mass m , e.g., $m = 0.1$, is rather small.

5. Conclusions

The fermion bag approach, Langevin dynamics and complex Langevin dynamics are used to solve the massive Thirring model at finite density in 0+1 dimension. The chiral condensate and fermion density by these methods are compared with the exact results. The complex Langevin dynamics only works for not too large interaction $U < O(1)$. Moreover, this method will also meet the computational difficulties when the fermion mass is too small, or the chemical potential is in the intermediate range $\mu = 1$. Since the sign problem is avoided in the Langevin dynamics and the fermion bag approach, these two methods can reproduce the exact results for a large range of parameters. Another advantage of the fermion bag approach over the Langevin dynamics is that a high computational efficiency are made for the strong interaction between fermions for the fermion bag approach. In the future paper we will check these advantages of the fermion bag approach over the other numerical methods for the massive Thirring model at finite density in 2+1 dimensions.

Acknowledgments. I would like to thank Prof. Shailesh Chandrasekharan for discussion. Daming Li was supported by the National Science Foundation of China (No. 11271258, 11571234).

References

- [1] G. Aarts, F.A. James, E. Seiler and I.-O. Stamatescu, Adaptive stepsize and instabilities in complex Langevin dynamics, Phys. Lett. B 687 (2010) 154, arXiv:0912.0617[hep-lat]

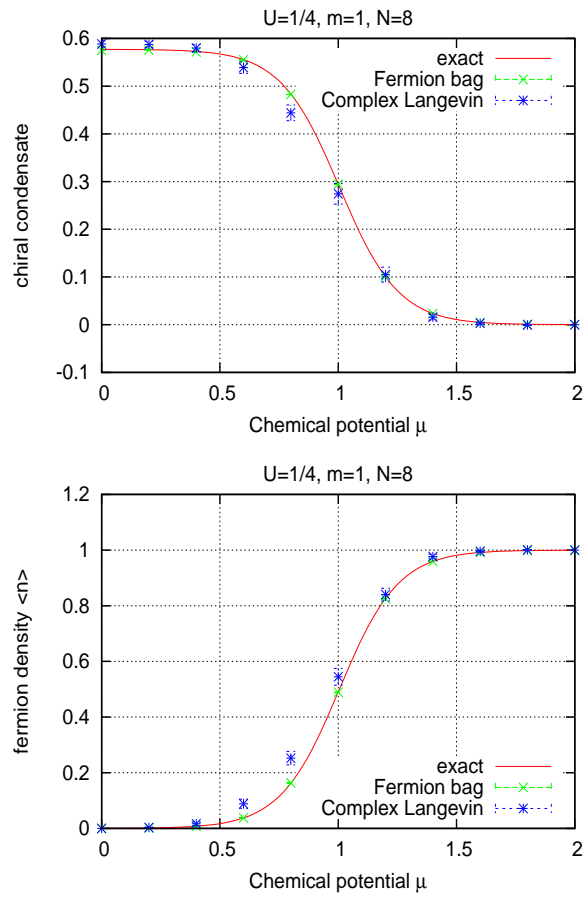


Figure 2: Comparison between Fermion bag approach, complex Langevin dynamics and exact solution.

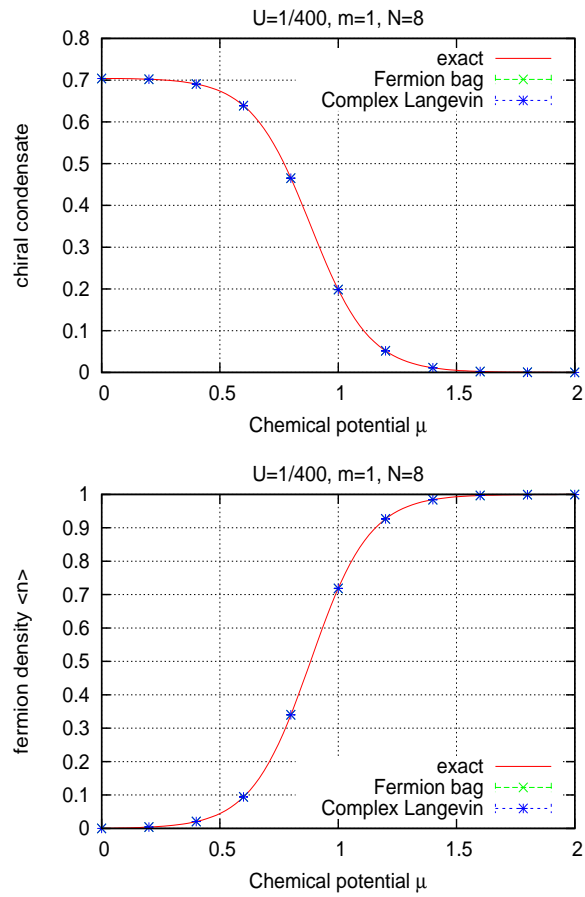


Figure 3: Comparison between Fermion bag approach, complex Langevin dynamics and exact solution.

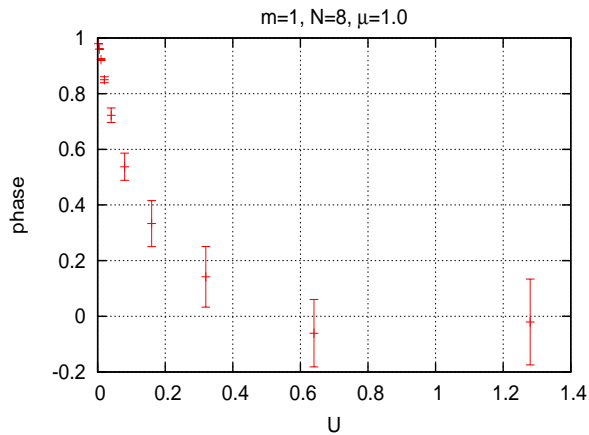


Figure 4: The dependence of phase $\langle e^{i\varphi} \rangle = \frac{Z}{Z_{\text{pq}}}$ on the fermion coupling strength $U = 0.0025, 0.005, 0.01, 0.02, 0.04, 0.08, 0.16, 0.32, 0.64, 1.28$, where Z_{pq} is the phase quenched approximation of Z in (15), $\Delta\Theta = 10^{-4}$, $t_{\text{equ}} = 40$, $t_{\text{end}} = 80$.

- [2] G. Aarts, Can stochastic quantization evade the sign problem? The relativistic Bose gas at finite chemical potential, Phys. Rev. Lett. 102 (2009) 131601, arXiv:0810.2089[hep-lat]
- [3] J. M. Pawłowski and C. Zielinski, Thirring model at finite density in 2 + 1 dimensions with stochastic quantization, Phys. Rev. D 87 (2013) 094509, arXiv:1302.2249[hep-lat]
- [4] J. Flower, S. W. Otto, and S. Callahan, Complex Langevin equations and lattice gauge theory, Phys. Rev. D 34, 598 (1986).
- [5] D. Sexty, Simulating full QCD at nonzero density using the complex Langevin equation, arXiv:1307.7748[hep-lat]
- [6] G. Aarts and I.-O. Stamatescu, Stochastic quantization at finite chemical potential, JHEP 09 (2008) 018, arXiv:0807.1597[hep-lat]
- [7] G. Aarts, F. A. James, J. M. Pawłowski, E. Seiler, D. Sexty and I. -O. Stamatescu, Stability of complex Langevin dynamics in effective models, JHEP 1303 (2013) 073, arXiv:1212.5231[hep-lat]
- [8] G. Aarts and F. A. James, Complex Langevin dynamics in the SU(3) spin model at nonzero chemical potential revisited, JHEP 01 (2012) 118, arXiv:1112.4655[hep-lat]
- [9] G. Aarts, L. Bongiovanni, E. Seiler, D. Sexty and I.-O. Stamatescu, Controlling complex Langevin dynamics at finite density, Eur. Phys. J. A 49 (2013) 89, arXiv:1303.6425[hep-lat]

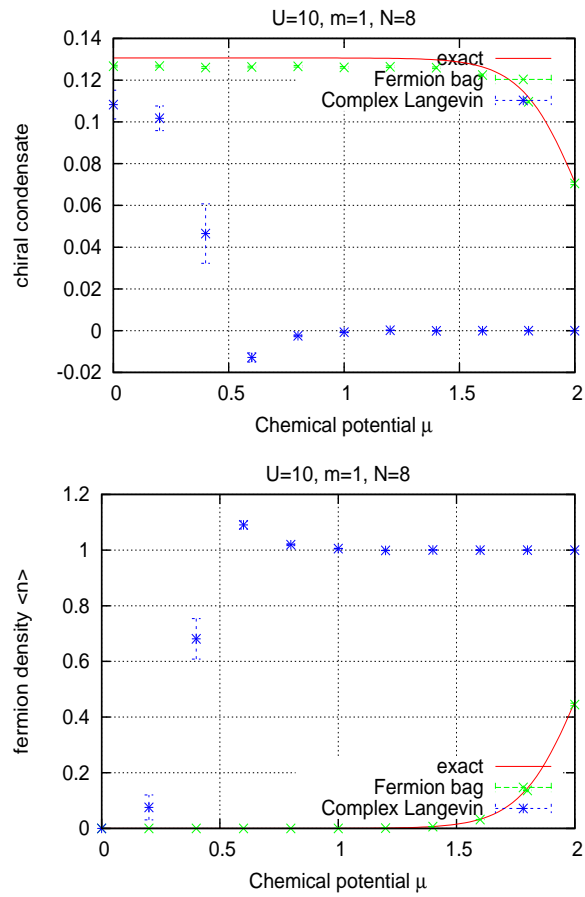


Figure 5: Comparison between Fermion bag approach, complex Langevin dynamics and exact solution.

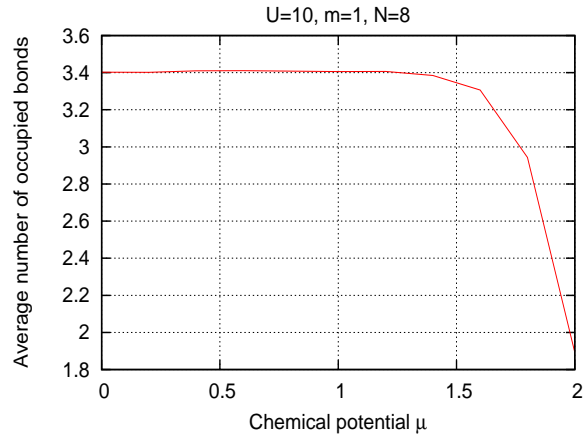


Figure 6: The average number of occupied bonds vs the chemical potential μ by fermion bag approach.

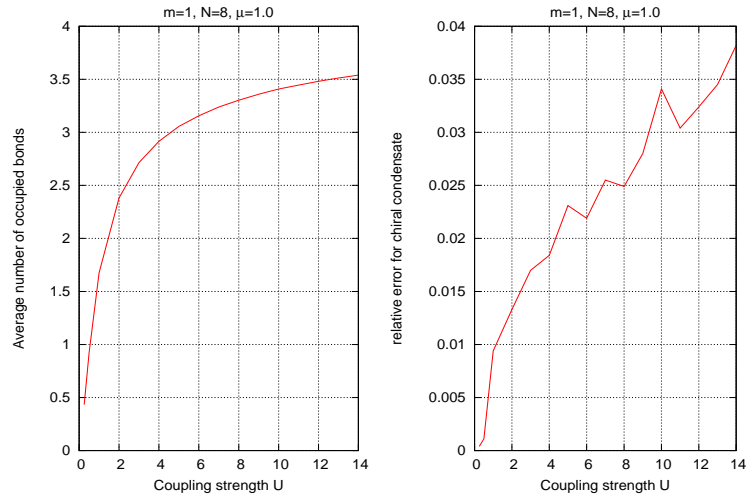


Figure 7: The average number of occupied bonds and relative error for chiral condensate vs the coupling strength U by fermion bag approach.

- [10] G. Aarts and F. A. James, On the convergence of complex Langevin dynamics: the three-dimensional XY model at finite chemical potential, JHEP 1008, 020 (2010), arXiv:1005.3468[hep-lat]
- [11] J. M. Pawłowski and C. Zielinski, Thirring model at finite density in 0+1 dimensions with stochastic quantization: Crosscheck with an exact solution, Phys.Rev. D87, 094503 (2013), arXiv:1302.1622[hep-lat]
- [12] H. W. Hamber and H. Ren, Complex probabilities and the Langevin equation, Phys. Lett. B 159, (1985) 330
- [13] J. Flower, S. W. Otto, and S. Callahan, Complex Langevin equations and lattice gauge theory, Phys. Rev. D 34, (1986) 598
- [14] E. -M. Ilgenfritz, Complex Langevin simulation of chiral symmetry restoration at finite baryonic density, Phys. Lett. B 181, (1986) 327
- [15] G. Aarts, F.A. James, E. Seiler and I.-O. Stamatescu, Eur. Phys. J. C 71 (2011) 1756 [arXiv:1101.3270] arXiv:1101.3270[hep-lat]
- [16] C. Gattringer and T. Kloiber, Lattice study of the Silver Blaze phenomenon for a charged scalar ϕ^4 field, Nucl. Phys. B 869, 56 (2013), arXiv:1206.2954[hep-lat]
- [17] Y. D. Mercado and C. Gattringer, Monte Carlo simulation of the SU(3) spin model with chemical potential in a flux representation, Nucl. Phys. B 862, 737 (2012), arXiv:1204.6074[hep-lat]
- [18] Y. D. Mercado, C. Gattringer, A. Schmidt, Surface worm algorithm for abelian Gauge-Higgs systems on the lattice, Comput. Phys. Commun. 184 (2013) 1535, arXiv:1211.3436[hep-lat]
- [19] C. Gattringer, T. Kloiber and V. Sazonov, Solving the sign problems of the massless lattice Schwinger model with a dual formulation, Nucl. Phys. B 897 (2015) 732, arXiv:1502.05479[hep-lat]
- [20] F. Bruckmann, C. Gattringer, T. Kloiber and T. Sulejmanpasic, Finite density O(3) non-linear sigma model and low energy physics, arXiv:1512.05482[hep-lat]
- [21] F. Bruckmann, C. Gattringer, T. Kloiber and T. Sulejmanpasic, Dual lattice representations for O(N) and CP(N-1) models with a chemical potential, Physics Letters B 749, 495 (2015), arXiv:1507.04253[hep-lat]
- [22] U. Wolff, Simulating the All-Order Strong Coupling Expansion III: O(N) sigma/loop models, Nucl. Phys. B 824 (2010) 254, arXiv:0908.0284[hep-lat]. U. Wolff, Nucl. Phys. B 834 (2010) 395 (Erratum).
- [23] U. Wolff, Simulating the All-Order Strong Coupling Expansion IV: CP(N-1) as a loop model, Nucl. Phys. B 832 (2010) 520, arXiv:1001.2231[hep-lat]

- [24] S. Chandrasekharan, Fermion Bag Approach to Fermion Sign Problems, New opportunities in lattice fermion field theories, Eur. Phys. J A49, 1 (2013), arXiv:1304.4900[hep-lat]
- [25] S. Chandrasekharan and A. Li, The generalized fermion-bag approach, PoS, LATTICE2011, 058 (2011), arXiv:1111.5276[hep-lat]
- [26] S. Chandrasekharan and A. Li, Fermion bag solutions to some sign problems in four-fermion field theories, PoS, LATTICE2012, 225 (2012), arXiv:1202.6572[hep-lat]
- [27] S. Chandrasekharan, Solutions to sign problems in lattice Yukawa models, Phys. Rev. D., 86, 021701, arXiv:1205.0084[hep-lat]
- [28] R. Oeckl and H. Pfeiffer, The dual of pure non-Abelian lattice gauge theory as a spin foam model, Nucl. Phys.B 598:400-426, 2001, arXiv:hep-th/0008095
- [29] J. W. Cherrington, D. Christensen, I. Khavkine, Dual Computations of Non-Abelian Yang-Mills on the Lattice, Phys. Rev. D 76 (2007) 094503, arXiv:0705.2629[hep-lat]
- [30] J. W. Cherrington, A Dual Algorithm for Non-abelian Yang-Mills coupled to Dynamical Fermions, Nucl. Phys. B794, 195 (2008), arXiv:0710.0323[hep-lat]
- [31] H. Pfeiffer, Exact duality transformations for sigma models and gauge theories, J. Math. Phys. 53, 033501 (2012);
- [32] U. Wolff, Monte Carlo Errors with less Errors, Comput. Phys. Commun. 156 (2004) 143-153, arXiv:hep-lat/0306017
- [33] L. G. Molinari, Determinants of block tridiagonal matrices, Linear Algebra and its Applications 429 (2008) 2221, arXiv:0712.0681[math-ph]

Appendix A. There is no sign problem for the presentation of Z by fermion bag approach in (7)

The $N \times N$ (even N) fermion matrix is

$$D = D(\mu, m) = \begin{pmatrix} m & \frac{e^\mu}{2} & & & & \frac{e^{-\mu}}{2} \\ -\frac{e^{-\mu}}{2} & m & \frac{e^\mu}{2} & & & \\ & -\frac{e^{-\mu}}{2} & m & \frac{e^\mu}{2} & & \\ & & & \ddots & & \\ & & & & m & \frac{e^\mu}{2} \\ -\frac{e^\mu}{2} & & & & -\frac{e^{-\mu}}{2} & m \end{pmatrix}_{N \times N}$$

According to a formula of the determinant [33], the determinant of D is

$$\det D = \frac{e^{N\mu}}{2^N} + \frac{e^{-N\mu}}{2^N} + \text{Tr}(T)$$

where the 2×2 transfer matrix T is $T = \begin{pmatrix} m & \frac{1}{4} \\ 1 & 0 \end{pmatrix}^N$. Obviously, $\det D > 0$ for any $\mu > 0$ and $m > 0$. Choose n different indices, $1 \leq i_1 < \dots < i_n \leq N$ and delete n rows and columns corresponding to these n indices from D to obtain \tilde{D} . We want to prove that $(N-n) \times (N-n)$ matrix \tilde{D} satisfies $\det \tilde{D} > 0$. This holds because the structure of \tilde{D} is the same with D and thus the determinant of \tilde{D} can be calculated [33], which must be positive. For example, $N = 10$, $n = 2$, $i_1 = 4$, $i_2 = 7$,

$$\tilde{D} = \begin{pmatrix} * & * & & | & & & | & & & * \\ * & * & * & | & & & | & & & \\ & * & * & | & & & | & & & \\ - & - & - & | & - & - & | & - & - & - \\ & & & | & * & * & | & & & \\ - & - & - & | & * & * & | & & & \\ & & & | & & & | & * & * & \\ * & & & | & & & | & * & * & * \\ & & & | & & & | & * & * & * \end{pmatrix}$$

Since $C(t_1, \dots, t_{2j})$ can be presented by the determinant of the submatrix of D , which is nonnegative, the sign problem is avoided for the presentation of Z by fermion bag approach in (7).